



Published in final edited form as:

*J Biomed Mater Res A*. 2011 October ; 99(1): 47–57. doi:10.1002/jbm.a.33162.

## Covalent stabilization of alginate hydrogel beads via Staudinger ligation: Assessment of poly(ethylene glycol) and alginate cross-linkers

Kerim M. Gattás-Asfura<sup>†</sup>, Christopher A. Fraker<sup>†,‡</sup>, and Cherie L. Stabler<sup>†,‡,\*</sup>

<sup>†</sup>Diabetes Research Institute, College of Engineering & Department of Surgery, Leonard M. Miller School of Medicine, University of Miami, 1450 N.W. 10<sup>th</sup> Avenue, Miami, FL 33136

<sup>‡</sup>Department of Biomedical Engineering, College of Engineering & Department of Surgery, Leonard M. Miller School of Medicine, University of Miami, 1450 N.W. 10<sup>th</sup> Avenue, Miami, FL 33136

### Abstract

Cellular encapsulation within alginate hydrogel capsules has broad applications in tissue engineering. In seeking to improve the inherent instability of ionically cross-linked alginate hydrogels, we previously demonstrated the covalent stabilization of Ba<sup>2+</sup> cross-linked alginate-azide beads via chemoselective Staudinger ligation using a 1-methyl-2-diphenylphosphino-terephthalate (MDT) terminated poly(ethylene glycol) linker. In this study, we functionalized variant PEG, linear and branched, and alginate polymers with MDT groups to evaluate the effect of size, structural design, number of functional groups, and charge on the resulting hydrogel bead. All cross-linkers resulted in enhanced covalent stabilization of alginate beads, with significant decreases in swelling and resistance to dissolution via Ba<sup>2+</sup> chelation. The MDT-functionalized alginate resulted in the most stable and homogeneous bead, with the most restrictive permeability even after EDTA exposure. Co-encapsulation of MIN6 cells within the cross-linked alginate hydrogel beads resulted in minimal effects on viability, whereas the degree of proliferation following culture varied with cross-linker type. Altogether, the results illustrate that manipulating the cross-linker structural design permits flexibility in resulting alginate beads characteristics. Covalent stabilization of alginate hydrogel beads with these chemoselective alginate and PEG-based cross-linkers provides a unique platform for cellular encapsulation.

### Keywords

Staudinger ligation; alginate; PEG; cross-linker design; encapsulation

## INTRODUCTION

Alginate is an attractive biopolymer for cellular encapsulation in tissue engineering applications.<sup>1</sup> It undergoes instant gelation following exposure to selected multivalent cations (e.g. Ca<sup>2+</sup>, Ba<sup>2+</sup>, and polycations).<sup>2</sup> This cross-linking mechanism, cation selectivity, and gelation efficiency have been studied in detail.<sup>3–4</sup> Since resulting alginate hydrogels are generally considered biocompatible and nonimmunogenic, these gels are being utilized to encapsulate cells within three-dimensional matrices<sup>2,5–6</sup>. Additional modifications of the

\*Corresponding Author: Phone (305) 243-9768; Fax (305) 243-4404; cstabler@miami.edu.

**Supporting Documents Available.** Detailed methods for polymer synthesis (where specified), characterization data, and other figures are outlined.

alginate backbone to enhance the compatibility of these gels for cellular encapsulation, such as through the attachment of cellular adhesion motifs, biodegradable linkers, and covalent cross-links, have been reported.<sup>7</sup>

One of the primary challenges associated with the use of alginate for cell-based research is the long term stability of these resulting gels following ionic cross-linking.<sup>8</sup> Maintenance of the structural integrity of the alginate gels is crucial for applications that require maintenance of gel properties *in vivo*, e.g. cellular immunoisolation. Therefore, methods for enhancing the stability of alginate hydrogels, particularly under ionic exchange conditions such as that seen *in vivo*, would be useful. We have previously reported the use of Staudinger ligation for achieving bioorthogonal and chemoselective covalent stabilization of alginate gels.<sup>9</sup> In order to achieve this, sodium alginate ( $M_w$  200–300) was functionalized with pendant alkyl azide groups utilizing a linear poly(ethylene glycol) (PEG) ( $M_w$  300) linker. The cross-linker consisted of linear PEG ( $M_w$  3400) having 1-methyl-2-diphenylphosphino-terephthalate (MDT) end groups. The spontaneous reaction between alkyl azide and MDT results in the formation of an amide bond.<sup>10</sup> Staudinger ligation is known for its benignity in the presence of live cells under physiological conditions, thus our covalent cross-linking approach was found to be compatible for encapsulation of mouse insulinoma (MIN6) cells, as well as pancreatic islets.<sup>11</sup> In working with these modified polymers, we noted two imperfections that we sought to resolve. First, we observed miscibility properties (e.g. cloudiness and phase separation) of the cross-linker in the presence of alginate-azide or cell culture media. Second, we found that a controlled pre-incubation time of the alginate-azide/cross-linker solutions was required prior to capsule formation via ionic gelation. Too long of a pre-incubation time increased the viscosity of the solution hindering bead fabrication, while too short of a pre-incubation time resulted in loss of the PEG polymer during the fabrication process.

Herein, the macromolecular structure of the cross-linker was redesigned to facilitate chemoselective covalent stabilization, while avoiding the above mentioned challenges during fabrication of the alginate-azide capsules. Hence, our original cross-linker (**1**) and three new ones (**2–4**) were investigated. These new cross-linkers were synthesized to vary in the number of 1-methyl-2-diphenylphosphino-terephthalate (MDT) end groups, net charge, molecular weight, and material composition. The chemical reactivity, solubility, and cytotoxicity of each cross-linker and resulting beads were compared. Pre-incubation time requirements for bead fabrication were determined. Additionally, covalent stabilization of the fabricated beads was evaluated via microscopic imaging and swelling in different solvents. Finally, the dynamic response of cells within these matrices was evaluated. Implications of these cross-linking schemes on enhancing alginate-based bead stabilization are discussed.

## MATERIALS AND METHODS

### Materials

Sodium alginates were all sourced from NovaMatrix. For fabrication of the alginate azide, a medium viscosity, high guluronic alginate was selected (PRONOVA UP MVG,  $M_w$  = 300 kDa,  $M_w/M_n$  = 1.87,  $DP_n$  of 28, Batch # FP-504-03). For cross-linker 4, a very low molecular weight, high guluronic sodium alginate was selected (PRONOVA UP VLVG,  $M_w$  = 28 kDa, G/M ratio = 2.03, Batch # BP-0711-09). The 1-ethyl-(dimethylaminopropyl) carbodiimide hydrochloride (EDC) was from Advanced Chemtech. Triethylamine was from Across Organics. Thin layer chromatography (TLC) was performed on Baker-flex Silica Gel IB-F cut into 12×25 mm sheets using 9/1 (v/v) of dichloromethane/methanol as developing solvent and  $I_2$  for spot visualization. The  $H_2N$ -4ArmPEG ( $M_w$  11,000 g/mol) and  $H_2N$ -PEG-tBoc ( $M_w$  3,600 g/mol) were from Laysan Bio, Inc. The silica gel (200–400 mesh, 60

Å) used for filtration, other solvents, and chemical reagents were from Sigma-Aldrich. The 3-(N-morpholino)propanesulfonic acid (MOPS) buffer consisted of 10 mM MOPS, 137 mM NaCl, 3 mM KCl, and pH 7.4 (adjusted with 6 M NaOH). The MOPS with Ba<sup>2+</sup> buffer consisted of 10 mM MOPS, 62 mM NaCl, 3 mM KCl, 0.20 mM tween-20, 50 mM BaCl<sub>2</sub>·2H<sub>2</sub>O, and pH 7.4 (adjusted with 6 M NaOH). This buffer was supplemented with 140 mM D-Mannitol for use with cells. The MOPS with sodium ethylenediaminetetraacetate (EDTA) buffer consisted of 10 mM MOPS, 12 mM NaCl, 3 mM KCl, 50 mM EDTA, and pH 7.4 (adjusted with 5 M HCl). Live/dead assay reagents were from Invitrogen and Hank's balanced salt solution (HBSS) without calcium or magnesium (Cellgro) was used as solvent. The 3-(4,5-dimethylthiazol-2-yl)-2,5-diphenyltetrazolium bromide (MTT) assay was from Invitrogen.

### Spectroscopic analysis

Attenuated total reflectance Fourier transform infrared (ATR-FT-IR) spectra were obtained utilizing the PerkinElmer Spectrum 100 FT-IR Spectrometer utilizing a KBr beam splitter, Universal ATR (1 bounce, Di/ZnSe) Sampling Accessory, and electronically, temperature-stabilized fast recovery deuterated triglycine sulfate (FR-DTGS) detector. Spectra were the average of 4 scans at a resolution of 4 cm<sup>-1</sup> or otherwise stated. UV-Vis measurements were obtained using the Molecular Devices SpectraMax M5 Microplate/Cuvette Reader. Proton nuclear magnetic resonance (<sup>1</sup>H-NMR) spectra were obtained using a 400 MHz Bruker NMR (located at the Chemistry Department, University of Miami, Coral Gables, FL) and tetramethylsilane (TMS) or 3-(trimethylsilyl)propionic-2,2,3,3-d<sub>4</sub> acid sodium salt (TSP) as reference standards with δ = 0.00 ppm. Processing and analysis of the <sup>1</sup>H-NMR spectra were performed using the MestRe-C 2.3a software. Samples prepared for fast atomic bombardment mass spectroscopic (FAB-MS, VG Trio2000) and matrix-assisted laser desorption/ionization time-of-flight mass spectrometric (MALDI-TOF-MS, Bruker Bi-Flex IV) analyses were submitted to the Chemistry Department of the University of Miami. For MALDI-TOF-MS, α-cyano-4-hydroxy-cinnamic acid was used as the matrix and 50% H<sub>2</sub>O/30% acetone/20% acetonitrile as the solvent. Confocal microscopic images were taken utilizing the Zeiss LSM510 microscope. Microscopic images of beads were taken utilizing the Carl Zeiss Axiovert 200 microscope. Multiple beads were imaged by the Olympus SZX7 stereomicroscope.

### Synthesis of Azide-Alginate

Synthesis of the alginate-azide was performed as previously reported with some minor modifications.<sup>9</sup> In brief, 100 mg of UP MVG sodium alginate, 28 mg N-hydroxysuccinimide (NHS) and 124 mg 2-(N-morpholino)ethanesulfonic acid was dissolved in 10 mL de-ionized water. A 200 μL solution of 377 mM N<sub>3</sub>-PEG-NH<sub>2</sub> (M<sub>w</sub> 372 g/mol) was added, followed by 116 mg 1-ethyl-(dimethylaminopropyl)carbodiimide hydrochloride (116 mg, 0.60 mmol), 25 min stirring, and drop-wise addition of 55 μL of 6 M NaOH. Purification was achieved via 4 days dialysis (10,000 MWCO membrane) against 600 mL water, which was changed three times a day. During the first 3 days, NaOH (10 μL of 6 M) and NaCl (400 μL of 4.26 M) were added twice daily to the alginate-containing solution. Larger batch sizes (10x) were also fabricated using this method. The remaining solution was filtered through a 0.2 μm membrane (Pall Corp) and freeze-dried. Purity and functionalization has been reported previously<sup>9</sup>, where purity was a minimum of 97 %, with an average azide modification of 11 % (percent modification of alginate carboxylate groups) or 149 N<sub>3</sub> per alginate mol ratio.

### Synthesis of linear MDT-PEG (1)

Synthesis of this cross-linker has been published previously.<sup>9</sup> In brief, 0.145 mmol N,N'-Diisopropylcarbodiimide (DIC) was added to a solution of 52.8 mg 1-methyl-2-

diphenylphosphino-terephthalate (MDT) (synthesis reported elsewhere<sup>9</sup>) and 17.2 mg N-hydroxysuccinimide (NHS) in 1.2 mL anhydrous/Ar-flushed N,N-dimethylformamide (DMF). The following agents were added at the time intervals indicated: 200 mg NH<sub>2</sub>-PEG-NH<sub>2</sub> (M<sub>w</sub> 3,513 g/mol) at 30 min and 14.8 mg 4-dimethylaminopyridine at 1 h. After reacting for 3 h under Ar atmosphere, the product was precipitated with 12 mL cold diethyl ether (Et<sub>2</sub>O) and collected by centrifugation at 0 °C. It was “crystallized” once in 10 mL 200 proof ethanol (warmed to 37 °C to dissolve, cooled in ice-water bath to precipitate, collected precipitate by centrifugation at 0 °C). The precipitate was washed once with 12 mL Et<sub>2</sub>O at 0 °C and dried under reduced pressure. Purity and functionalization of cross-linker 1 has been reported previously<sup>9</sup>, where purity was a minimum of 99 %, with > 97 % conversion of end groups to MDT.

### Synthesis of 4ArmPEG-MDT (2)

MDT (52.8 mg, 0.145 mmol, synthesized as previously reported<sup>9</sup>) and N-hydroxysuccinimide (NHS, 17.2 mg, 0.147 mmol) were dissolved in 1.2 mL anhydrous N,N-dimethylformamide (DMF) utilizing a 15 mL polypropylene (pp) centrifuge tube. To this solution, N,N'-diisopropylcarbodiimide (DIC, 22.5 μL, 0.145 mmol) was added and mixed with vortex for 30 min. Subsequently, 4ArmPEG-NH<sub>2</sub> (300 mg, 0.027 mmol) was added and mixed with vortex for an additional 30 min. Finally, 4-dimethylaminopyridine (DMAP, 14.8 mg, 0.121 mmol) was added and mixed with vortex for an additional 60 min. All steps were performed at room temperature (RT, 22±2 °C) under Ar atmosphere. To collect and purify the product, it was precipitated by mixing with 10 mL cold (ice-water bath) diethyl ether (Et<sub>2</sub>O) and collected by centrifugation (3500 rpm, 5 min, 0 °C). Then, it was dissolved in 10 mL ethanol (EtOH, 200 proof) at 37 °C, cooled in ice-water bath to precipitate, and collected by centrifugation as described above. Finally, it was washed once with 10 mL cold Et<sub>2</sub>O and dried under reduced pressure. Yield: 309 mg. Appearance: white to light yellow solid powder. Kaiser's test: negative. TLC: single spot (R<sub>f</sub> 0.43). Selected characteristic ATR-FT-IR bands: 2884 (ν<sub>s</sub>, C-H, PEG), 1719, 1660 (ν, C=O, amide I), 1538 (δ, N-H, amide II), 1102 (ν<sub>s</sub>, C-O, PEG), 749 (MDT), and 699 (MDT) cm<sup>-1</sup>. <sup>1</sup>H-NMR (CDCl<sub>3</sub> with 0.03 % v/v TMS): δ 3.404–3.832 (m, 1018H) and 7.275–8.290 (m, 52H) ppm with 96 % purity. M<sub>w</sub> by MALDI-TOF-MS: 11,915 g/mol.

### Synthesis of MDT-Asp-4ArmPEG (3)

Synthesis was achieved via a two stage process. First (step **A**), H<sub>2</sub>N-Asp(OtBu)-4ArmPEG (165 mg, 0.014 mmol, synthesized as described in Supporting Documents, Asp refers to aspartic acid) and MDT-NHS (34 mg, 0.093 mmol, synthesized as previously reported<sup>9</sup>) were dissolved in 700 μL anhydrous DMF utilizing a 15 mL pp centrifuge tube. To this solution, DMAP (7 mg, 0.057 mmol) was added and mixed with vortex until fully dissolved. Then, triethylamine (TEA, 32 μL, 0.230 mmol) was added and mixed with vortex for 3 h followed by overnight incubation. All steps were performed at RT under Ar atmosphere. The product was collected and purified as described for **2** except that only 6 mL of EtOH were used instead. Yield: 165 mg. Appearance: white to light green solid powder. Kaiser's test: negative. TLC: single spot (R<sub>f</sub> 0.39). Selected characteristic ATR-FT-IR bands: 2883 (ν<sub>s</sub>, C-H, PEG), 1721, 1665 (ν, C=O, amide I), 1533 (δ, N-H, amide II), 1101 (ν<sub>s</sub>, C-O, PEG), 748 (MDT), and 699 (MDT) cm<sup>-1</sup>. <sup>1</sup>H-NMR (CDCl<sub>3</sub> with 0.03 % v/v TMS): δ 1.448 (s, 36H), 3.424–3.841 (m, 1033H), and 7.298–8.126 (m, 73H) ppm with 95 % purity.

Subsequently (step **B**), for removal of the OtBu carboxyl-protecting groups, MDT-Asp(OtBu)-4ArmPEG (above product, 145 mg, 0.011 mmol) was reacted with 420 μL anhydrous dichloromethane, 35 μL triisopropylsilane, and 245 μL trifluoroacetic acid for 2 h (at RT and under Ar atmosphere) utilizing a 15 mL pp centrifuge tube and vortex for mixing. The product was precipitated by mixing with 10 mL cold Et<sub>2</sub>O, collected by

centrifugation (3500 rpm, 5 min, 0 °C), and dried under reduced pressure. It was washed once more with 10 mL cold Et<sub>2</sub>O and dried under reduced pressure. The deprotection and precipitation with Et<sub>2</sub>O steps above were repeated once more. Then, the resulting dried precipitate was dissolved in 400 μL anhydrous DMF and mixed well with TEA (37 μL, 0.270 mmol). The product was purified as described in the step A above. Then, it was dissolved in 1 mL purified water, passed through a 4 mL (12×35mm) column of SP Sephadex C-25 using water as solvent, and freeze-dried. Yield: 85 mg. Appearance: yellowish-green to white solid powder. TLC: single spot (R<sub>f</sub> 0.11). Selected characteristic ATR-FT-IR bands: 2882 (ν<sub>s</sub>, C-H, PEG), 1720, 1662 (ν, C=O, amide I), 1533 (δ, N-H, amide II), 1097 (ν<sub>s</sub>, C-O, PEG), 749 (MDT), and 699 (MDT) cm<sup>-1</sup>. <sup>1</sup>H-NMR (CDCl<sub>3</sub> with 0.03 % v/v TMS): δ 1.447 (s, 7H), 3.424–3.841 (m, 810H), and 7.320–8.095 (m, 73H) ppm with 95 % purity and 75 % degree of deprotection. M<sub>w</sub> by MALDI-TOF-MS: 12,252 g/mol.

#### Synthesis of Alg-MDT (4)

H<sub>2</sub>N-PEG-MDT (50 mg, 11.9 μmol, synthesized as described in Supporting Documents), 2-(N-morpholino)ethanesulfonic acid (MES, 19 mg, 89.1 μmol), sodium alginate (PRONOVA UP VLVG, 15 mg, 0.5 μmol), and NHS (5 mg, 43.0 μmol) were dissolved in 2 mL of purified water utilizing a 15 mL pp centrifuge tube. To this solution, solid EDC (40 mg, 207.6 μmol) was added and mixed with vortex for 25 min. Then, pH was slowly adjusted to 8.5–9.0 (pH paper) with 6 M NaOH (≈ 18 μL, 1 μL/min) and mixing continued for additional 15 min. All steps were performed at RT and under Ar atmosphere. The product was purified by dialysis for 6 h utilizing a 10,000 MWCO membrane against 400 mL purified water (replaced every 10 min under constant degassing with Ar). During the first 4 h, 60 μL of NaCl (4.2 M)/NaOH (0.1 M) solution was added to the alginate solution (within the membrane, final pH<sub>paper</sub> 8.0) every 30 min and mixed well with a plastic pipet. The dialyzed solution was filter-sterilized (0.20 μm membrane) and freeze-dried. Yield: 47 mg. Appearance: brownish-white, solid, foamy material. Selected characteristic ATR-FT-IR bands: 3343 (ν, O-H), 2883 (ν<sub>s</sub>, C-H, PEG), 1721, 1652 (ν, C=O, amide I), 1613 (ν<sub>as</sub>, CO<sub>2</sub><sup>-</sup>), 1547 (δ, N-H, amide II), 1100 (ν<sub>s</sub>, C-O, PEG), 748 (MDT), and 699 (MDT) cm<sup>-1</sup>. M<sub>w</sub> by <sup>1</sup>H-NMR: 91,838 g/mol with a 15 MDT/alginate mol ratio.

#### Synthesis of CH<sub>3</sub>-PEG-MDT and CH<sub>3</sub>-PEG-N<sub>3</sub>

For FT-IR analysis, CH<sub>3</sub> and MDT or N<sub>3</sub> terminated linear PEG polymers were fabricated from CH<sub>3</sub>-PEG-NH<sub>2</sub> (M<sub>w</sub> 5,000 g/mol). For CH<sub>3</sub>-PEG-MDT fabrication, CH<sub>3</sub>-PEG-NH<sub>2</sub> (200 mg, 0.04 mmol), MDT-NHS (23 mg, 0.05 mmol), and triethylamine (17 μL, 0.12 mmol) were reacted in 500 μL anhydrous DMF utilizing a 15 mL pp centrifuge tube. After mixing with vortex for 25 min (at RT and under Ar atmosphere), the product was purified as described for **2** except that only 7 mL of EtOH was used instead. Yield: 191 mg. Appearance: white, solid powder. Kaiser's test: negative. TLC: single spot (R<sub>f</sub> 0.33). Selected characteristic ATR-FT-IR bands: 2884 (ν<sub>s</sub>, C-H, PEG), 1720, 1664 (ν, C=O, amide I), 1537 (δ, N-H, amide II), 1099 (ν<sub>s</sub>, C-O, PEG), 750 (MDT), and 700 (MDT) cm<sup>-1</sup>. <sup>1</sup>H-NMR (CDCl<sub>3</sub> with 0.03 % v/v TMS): δ 3.380 (s, 3H), 3.452–3.831 (m, 467H), and 7.281–7.384 (m, 4H) ppm with 95 % purity. M<sub>w</sub> by MALDI-TOF-MS: 5,331 g/mol.

For CH<sub>3</sub>-PEG-N<sub>3</sub> fabrication, CH<sub>3</sub>-PEG-NH<sub>2</sub> (200 mg, 0.04 mmol), NHS-PEG-N<sub>3</sub> (41 mg, 0.05 mmol, M<sub>w</sub> 914 g/mol, synthesized as described in Supporting Documents), and TEA (17 μL, 0.12 mmol) were dissolved in 500 μL anhydrous DMF utilizing a 15 mL pp centrifuge tube. After mixing with vortex for 25 min (at RT and under Ar atmosphere), the product was purified as described for CH<sub>3</sub>-PEG-MDT. Yield: 203 mg. Appearance: white, solid powder. Kaiser's test: negative. TLC: single spot (R<sub>f</sub> 0.32). Selected characteristic ATR-FT-IR bands: 2882 (ν<sub>s</sub>, C-H, PEG), 2105 (ν<sub>as</sub>, N<sub>3</sub>), 1738, 1665 (ν, C=O, amide I),



1543 ( $\delta$ , N-H, amide II), and 1096 ( $\nu_s$ , C-O, PEG)  $\text{cm}^{-1}$ .  $^1\text{H-NMR}$  ( $\text{CDCl}_3$  with 0.03 % v/v TMS):  $\delta$  2.224 (t, 2H, J: 6.8, 7.6 Hz), 3.372 (s, 3H), and 3.422–3.822 (m, 524H) ppm with 96 % purity.  $M_w$  by MALDI-TOF-MS: 5,347 g/mol.

### Quantification of MDT content on cross-linker 4 by $^1\text{H-NMR}$

A calibration curve was obtained by plotting the  $^1\text{H-NMR}$  peak area ratio between PEG ( $\delta$  3.72 ppm) and 3-(trimethylsilyl)propionic-2,2,3,3- $\text{d}_4$  acid sodium salt (TSP, 0.05 wt%,  $\delta$  0.000 ppm) as a function of  $\text{H}_2\text{N-PEG-MDT}$  concentration (from 0.06 to 0.48  $\mu\text{mol}$  range) in  $\text{D}_2\text{O}$  (see Figure 1 in Supporting Documents). Untreated sodium alginate (PRONOVA UP VLVG, 0.07 % wt/v) was added to all the samples. Degree of functionalization for **4** at 0.27 % wt/v was interpolated from the linear fit of the calibration curve.

### Quantification of Staudinger ligation efficiency

Alginate-azide or each cross-linker was reacted with  $\text{CH}_3\text{-PEG-MDT}$  or  $\text{CH}_3\text{-PEG-N}_3$ , respectively in MOPS buffer at equimolar concentrations (5 mM) of functional groups. Reactivity was correlated to the area of the  $\text{N}_3$  IR band (2194–2033  $\text{cm}^{-1}$ ) as a function of time at 37 °C. These quantitative FT-IR measurements were performed using a 0.1 mm ZnSe transmission sealed flow cell, scan range of 2350–1850  $\text{cm}^{-1}$ , and 4  $\text{cm}^{-1}$  resolution. A fresh sample aliquot (70  $\mu\text{L}$ ) was collected for each reading. Sample solutions were stirred every 30 min during the experiment. Centrifugation was used to remove air bubbles. Background correction was performed using a buffer-filled ZnSe cell. The number of scans or re-initializing spectra collection varied until reaching similar straight baselines for accurate measurements. Data processing included one automatic baseline correction and smoothing. After each reading, the cell was cleaned three times with 3 mL water, once with 2 mL EtOH, and Ar-flushed to dry.

### Fabrication of hydrogel beads

The concentration of each polymer was kept constant at 1.5 % wt/v in Dulbecco's modified Eagle's medium (DMEM). For cellular encapsulation, the polymer mixture was added to cell pellets and gently mixed for a final density of  $2\text{E}+07$  cells/mL, as outlined in Scheme 1. A parallel air flow bead generator (Biorep, Inc. Miami, FL) was used to fabricate the beads in  $\text{Ba}^{2+}$  containing MOPS buffer and a 10 min gelation period. Cell-free beads were rinsed twice in MOPS buffer without  $\text{Ba}^{2+}$  and incubated in MOPS buffer until further assessment. Cell-filled beads were rinsed with 1X HBSS (Hank's buffered salt solution) with  $\text{Ca}^{2+}$  and  $\text{Mg}^{2+}$  (Invitrogen), transferred to 6 well plates (50 beads/well) and cultured in 2 mL DMEM culture media in a humidified 37 °C, 5 %  $\text{CO}_2$  / 95 % air incubator. Beads prepared with crosslinker **1**, **2**, **3**, or **4** had average diameters of  $917\pm 59$ ,  $945\pm 31$ ,  $922\pm 43$ , or  $956\pm 48$   $\mu\text{m}$  respectively.

### Cell Viability and Metabolic Assessment

MTT and live/dead assays were performed on capsules containing mouse insulinoma MIN6 cells. Prior to encapsulation, MIN6 cells (passage 53 to 63) were cultured as monolayers in T-flasks and fed every 2–3 days with fresh DMEM medium supplemented with 10 % fetal bovine serum (FBS; Sigma), 1 % penicillin-streptomycin (P/S), 1 % L-glutamine, and 0.001 % (v/v)  $\beta$ -mercaptoethanol. Cell-loaded beads (12-well plate, triplicates,  $n = 30$ ) were incubated in MTT solution (0.5 mg/mL in DMEM) for 3 h in the incubator. Excess media was removed followed by addition of 1 mL dimethyl sulfoxide (DMSO) to terminate the reaction. After 15 min shaking, the solutions were diluted by half with DMSO in 96-well plates and the absorbance of the final 200  $\mu\text{L}$  solution was read at 570 nm. Cell number was extrapolated from a standard curve of MIN6 cells. Live/dead assay (Invitrogen) consisted of

rinsing the cell-loaded beads twice with HBSS following incubation in 200  $\mu\text{L}$  of the live (green, 4  $\mu\text{M}$ ) and dead (red, 8  $\mu\text{M}$ ) stains in HBSS for 1 h at 37  $^{\circ}\text{C}$ .

### Statistical Analysis

Reported significant differences were based on one-way analysis of variance (ANOVA,  $\alpha$  of 0.05) followed by pair-wise means comparisons with Tukey's Honestly Significant Difference (HSD) Post Hoc test.

## RESULTS AND DISCUSSION

### Synthesis and characterization of functionalized polymers

All four cross-linkers tested (see Figure 1 for summary) were successfully synthesized via amide bonding assembly.  $^1\text{H-NMR}$  spectroscopy and TLC revealed cross-linker purities of 95 %. The Kaiser's test was utilized to ensure complete reaction of the primary amino groups.<sup>12</sup> ATR-FT-IR validated the functional groups on the cross-linkers, including amide bond formation by appearance of the amide I and II IR bands centered at approximately 1661 and 1543  $\text{cm}^{-1}$ , respectively. Weight-average molecular weights ( $M_w$ ) and degree of functionalization of alginate-azide (Alg- $\text{N}_3$ ) and cross-linkers (**1–4**) are summarized in Table 1.  $M_w$  values were determined by MALDI-TOF-MS except for **4**, which was calculated based on its degree of modification (15 MDT/alginate mol ratio, 10 % of carboxylate groups) by  $^1\text{H-NMR}$  analysis. In order to maintain equimolar amounts of MDT and azide groups, the weight of cross-linker **1**, **2**, **3**, or **4** added should be 1.0, 1.5, 1.6, or 3.1 times the weight of Alg- $\text{N}_3$  (Table 1,  $M_w$ /functional group ratio).

### Reactivity of Alg- $\text{N}_3$ and cross-linkers

The reaction between the azide and MDT functional groups on the polymers fabricated was measured via FT-IR spectroscopy by quantifying the decrease in the area of the azide IR band (centered at 2121  $\text{cm}^{-1}$ ) over time.<sup>9</sup> The results are shown in Figure 2. In the absence of MDT groups, the area of the  $\text{N}_3$  IR band remained constant, indicating stable azide groups under the experimental conditions. All cross-linkers had similar reaction kinetics, with the following general reactivity trend of 26, 47, 62, and 70 % after 1, 3, 5, and 7 h, respectively. The reaction started to plateau at 5 h, with no statistically significant change in the area of the  $\text{N}_3$  band, indicating completion of reaction at 5 h. In contrast, Alg- $\text{N}_3$  reached 18, 31, 43, and 49 % completion at the same respective incubation time, but also reached completion at 5 h. These results confirm that the MDT end groups on the cross-linkers can react with the azide groups on Alg- $\text{N}_3$ . Of note, linear monofunctional PEG polymers were used as complimentary cross-reactive polymers in this study to prevent gel formation during analysis. Therefore, this test provides only a general trend of end group reactivity.

### Miscibility properties of functionalized polymers

While cross-linker **1** dissolved readily in MOPS buffer, it formed cloudy solutions and phase separated in the presence of Alg- $\text{N}_3$  or DMEM. Similar miscibility properties were also observed for the four-arm PEG cross-linker **2** (see Figure 2 of Supporting Documents). Both cross-linkers present the hydrophobic MDT as end groups, which might impart the observed miscibility properties. For this reason, cross-linker **3** was designed to incorporate a charged group near the MDT, via the addition of aspartic acid (Asp) as part of the end group. Introduction of Asp moieties was successfully accomplished following the use of protected Asp and Fmoc solid-phase peptide synthesis/deprotection protocols.<sup>13</sup> Similarly, other specialized linkers (e.g. for cell binding, enzymatic hydrolysis, and different chemoselective reactions) could be incorporated for additional functionalities. The Asp moiety, with its carboxylate side chain, modified the solubility properties of **3**, as visualized by the lack of

cloudiness and phase separation in the presence of Alg-N<sub>3</sub> and DMEM at 1.5 % wt/v (see Supporting Documents). Cross-linker **4** yielded clear solutions in water, MOPS buffer, and DMEM, even in the presence of Alg-N<sub>3</sub>, at the same 1.5 % wt/v (see Supporting Documents).

**Beads fabrication and covalent stabilization**—In order to maintain the same 3 % wt/v total polymer concentration of Alg-N<sub>3</sub> with crosslinker solutions, alginate control consisted of 1.5 % alginate (MVG) and 1.5 % alginate (VLVG) wt/v. All polymer solutions were made in full culture media to take full advantage of the chemoselective nature of the ligation scheme. The air flow in the coaxial bead generator was adjusted to obtain spherical and homogeneous beads with diameters of 1.0±0.1 mm (Figure 3). For each cross-linker study, the Alg-N<sub>3</sub> plus cross-linker solution was pre-incubated for different time periods prior to fabrication of the beads, see Scheme 1 for summary. For all cross-linkers, solution viscosity increased with increasing polymer pre-incubation time. Significant increases in solution viscosity would subsequently prevent fabrication of spherical and uniform beads. The maximum pre-incubation time for each cross-linker to permit bead production was determined to be 40 min for cross-linker **1** and 20 min for cross-linkers **2–4**.

At higher magnification, Alg-N<sub>3</sub> and Alg-N<sub>3</sub>+**4** beads presented clear and homogeneous topographies (Figure 3). The control alginate beads presented less homogeneous topography. And, Alg-N<sub>3</sub> with cross-linker **1**, **2**, or **3** presented a corrugated topography. This may be indicative of the introduction of “defects” due to the inability of the PEG-based polymers to undergo ionic cross-linking and the resulting covalent bonding of cross-linkers **1**, **2**, and **3**. Defect visualization was likely minimized with the use of **4**, as a consequence of its alginate backbone and capacity for ionic cross-linking. Similar alginate/PEG bead topographies have been reported in the literature. These reports revealed that in the presence of PEG, macropore networks can be formed within the alginate beads and allow for high-density growth of mammalian cells with minimal cell leakage.<sup>14</sup>

Stability of the different bead formulations was evaluated via assessment of degree of swelling upon equilibration in water, EDTA buffer, or DMEM (Figure 4). For water or EDTA studies, the bead bathing solution was replaced three times (45 min incubation period between washes) prior to measurement of bead swelling, which is reported as the percent change in bead diameter from its baseline size (beads prior to washing). Control alginate and Alg-N<sub>3</sub> beads exhibited considerable swelling and subsequent breakage in water (Supporting Documents, Figure 3), thereby preventing swelling assessment. Addition of any of the four chemoselective cross-linkers resulted in mechanically stable beads, demonstrating the significant enhancement in bead stability observed with the incorporation of chemoselective covalent cross-links (Figure 4A). With the exception of beads cross-linked with **4**, pre-incubation of the Alg-N<sub>3</sub> with cross-linker **1**, **2**, or **3** resulted in a significant decrease in swelling (Figure 4A). This trend was observed until the viscosity of the solution prevented bead fabrication, i.e. 40 min for cross-linker **1** and 20 min for cross-linkers **2–4**. Results indicate that the pre-incubation time permits the initiation of cross-linking between the polymers, thereby reducing leach out of the cross-linker following bead fabrication. The incorporation of the alginate backbone in **4** eliminated the need for pre-incubation to enhance bead stability, as demonstrated by the insignificant changes in bead swelling with pre-incubation. This suggests that the loss of cross-linker **4** following bead fabrication and washing is minimal, which is likely due to the ability of the alginate backbone to undergo ionic cross-linking. To prove the presence of covalent cross-linking within the resulting beads, beads were equilibrated in EDTA buffer to remove all ionic interactions. Subsequently, bead diameters were measured, see Figure 4B. For crosslinkers **1** and **3**, covalent stabilization was not observed at pre-incubation time of 0 min, as the resulting beads ruptured; however, covalent stability was observed when a > 15 min pre-incubation



time was introduced prior to bead formation. Cross-linker **2** offered moderate stabilization of Alg-N<sub>3</sub> beads without pre-incubation, likely due its branched structure and observed solubility properties. Enhanced stability of beads cross-linked with polymer **2** was observed with increasing pre-incubation times. Beads cross-linked with polymer **4** were found to be the most stable of all groups, with only a 24 % increase in bead diameter, even without pre-incubation. Pre-incubation of alginate with cross-linker **4** resulted in no significant changes in bead swelling, indicating that the formation of cross-links prior to bead fabrication did not enhance resulting bead stability. These results further confirm that the loss of polymer **4** following fabrication of beads is minimal.

Since we anticipate applications of these polymers in cellular encapsulation, the swelling of resulting beads in DMEM culture medium was studied for 14 days. Beads were pre-incubated in DMEM for 2 h prior to Day 0 assessment. Percent swelling was compared to Day 0 measurements. The culture medium was replaced at each time point. Pre-incubation times used in this swelling study were 30, 20, 15, and 0 min for cross-linkers **1**, **2**, **3**, and **4**, respectively. Alginate control beads maintained almost a constant bead size throughout the test period, with a maximum swelling of 4 %. In contrast, Alg-N<sub>3</sub> beads with no cross-linker increased in diameter by 7, 15, 22, and 48 % after 2, 4, 7, and 10 days, respectively (Figure 4C). After 10 days, beads became soft, and broke apart during handling and rinsing cycles. This indicates that the functionalization reaction modified the resulting ionic cross-linking network of the alginate. This result is not surprising, taking into consideration that carboxylate groups are being used to link the azide groups and the azide group is introduced via a 600 MW PEG molecule. Similar swelling and stability properties of hydrogels consisting of functionalized alginate via carbodiimide chemistry have been reported in the literature including a correlation with degree of functionalization.<sup>15</sup> In this context, the stability of Alg-N<sub>3</sub> beads was greatly improved in the presence of a cross-linker (Figure 4C), where a maximum swelling of 20, 10, 16, and 15 % for **1**, **2**, **3**, and **4**, respectively, was observed after 14 days. Beads underwent statistically significant swelling within the first 4 days, followed by a plateau until day 7–10 and further swelling at day 14 (Figure 4C). Some factors that influence the swelling response of alginate hydrogels are the alginate characteristics, gelation process/conditions, temperature, and ion environment.<sup>16</sup> Hence, the observed swelling of the beads upon changing the equilibration buffer from MOPS to DMEM may be attributed to changes in the ion environment.

It was also noticed that Ba<sup>2+</sup>-cross-linked alginate beads deformed and remained deformed upon gentle compression. On the contrary, covalently cross-linked alginate-azide beads were more resistance to deformation upon compression (Figure 4D). Previous stress-relaxation studies for alginate hydrogels have shown that ionically cross-linked alginate gels relax a stress through breaking and subsequent reforming of the ionic cross-links, while covalently cross-linked alginate gels relax the stress through migration of water.<sup>17</sup> This could explain the observed deformation characteristics of the different beads.

### Permeability properties of beads

The permeability of the beads (prepared as in DMEM swelling experiment, n = 3) was evaluated via incubation in containing fluorescently-labeled dextran (FITC-dextran) of different M<sub>w</sub> at 0.1 mg/mL in MOPS buffer. All beads were thoroughly rinsed and equilibrated in MOPS buffer prior to permeability testing. Single 50 μm deep planar confocal images were utilized to visualize diffusion of FITC-dextran within the beads. Imaging parameters were kept consistent between polymer combinations for each molecular weight dextran. Gradient-type fluorescence intensity was observed (Figure 5). Visually, fluorescent intensity within the beads decreased with increasing M<sub>w</sub> of FITC-dextran in the range of 10–500 kDa. The fluorescence intensity within the Alg-N<sub>3</sub> beads stabilized with **1**,

2, and 3 was not homogeneous, which is in agreement with observed microscopic topographies described above for these beads. Overall, beads pre-incubated with EDTA were observed to illustrate a higher overall fluorescence.

Metamorph analysis (Universal Imaging Corporation software) on beads verified these visual assessments. Fluorescent intensity within the beads were quantified for each polymer combination and compared to alginate controls. At 40 and 150 kDa dextran, beads cross-linked with polymers 1–3 exhibited a higher fluorescent intensity within the bead than alginate controls, which is likely due to the inhomogeneity of the resulting hydrogel network. At 250 kDa dextran, there was no measurable difference between the polymer combinations and the alginate control, with the exception of the Alg-N<sub>3</sub>+4 beads. Beads cross-linked with polymer 4 exhibited a substantial decrease in fluorescent intensity within the bead, when compared to alginate controls (> 60%). These results indicate that the permeability of these beads to compounds ~250 kDa is more restrictive. This could be advantageous for cellular encapsulation and in vivo implantation, given that this may lead to greater restriction of antibody diffusion.<sup>18</sup> For 500 kDa dextran, there was no measurable difference between any of the polymer combinations and the alginate control. Upon exposure to EDTA, beads cross-linked with polymers 1–3 exhibited a significant increase in fluorescent intensity for all dextran MWs. Alg-N<sub>3</sub>+4 beads exposed to EDTA, however, demonstrated no significant increase in fluorescence intensity when compared to untreated alginate controls. This data indicates that the permeability of Alg-N<sub>3</sub>+4 beads is similar to standard barium cross-linked alginate beads after being exposed to EDTA buffer. The resistance of Alg-N<sub>3</sub>+4 microbeads to alterations in permeability with the removal of ionic interactions makes it highly desirable to cellular encapsulation, particularly for long term implantation.

### Viability and metabolic activity of MIN6 cells with the polymers

MTT and live/dead assays were utilized to assess the polymer and dual crosslinking effect on viability and proliferation of encapsulated MIN6 cells. Supplemented DMEM medium was used as a solvent and each polymer was incorporated at 1.5% wt/v. A slight decrease in cell number/bead from initial loading density, 8 to 24 %, was observed for Alg-N<sub>3</sub>+2 and Alg-N<sub>3</sub>+3 beads at day 1, respectively (Figure 6A). Cell number recovered by day 3, indicating that this affect is transient. Longer incubation times resulted in cell proliferation within all the beads, with an increase from 1.4 to 6.3 fold observed for the various cross-linkers. By Day 14, all cross-linked alginate groups exhibit an increase in growth statistically different than alginate controls. Growth rate varied across beads groups and it is believed to be controlled by the physical properties of the beads (e.g. softness, swelling, and permeability). A general trend between increase in cell number and bead swelling in DMEM is observed, indicating a possible correlation between swelling and cell growth. Live/dead stain at day 7 found highly viable (green-fluorescent) cells within all polymer bead groups (Figure 6B). These results, coupled with permeability studies, indicate the mass transfer of nutrients into and out of all of the bead formulations is adequate to ensure cell survival and function. This is further supported by our previous work evaluating the glucose stimulated insulin secretion response for pancreatic islets encapsulated in alginate-azide cross-linked with linker 1, where glucose diffusion in and insulin diffusion out of the beads was similar to barium cross-linked alginate controls.<sup>11</sup>

## CONCLUSIONS

Multiple MDT end groups, introduction of polar charged moieties, size of polymers, and material composition manipulated the physical properties of the cross-linkers and expanded the capacity for covalent stabilization of Alg-N<sub>3</sub> beads via Staudinger ligation. Branched

PEG polymers were found to reduce the loss of cross-linker following bead fabrication, although this effect was mitigated when polymer miscibility was enhanced. The beads supported growth of MIN6 cells at variable rates depending primarily on the polymeric composition of the bead. Results indicate that an alginate-based cross-linker may be the most desirable, given its high miscibility and lack of pre-incubation time for formation of covalently stabilized beads.

## Supplementary Material

Refer to Web version on PubMed Central for supplementary material.

## Acknowledgments

This work was supported by the National Institutes of Health through the Type 1 Diabetes Pathfinder Award Program (1DP2 DK08309601), the Diabetes Research Institute Foundation ([www.diabetesresearch.org](http://www.diabetesresearch.org)), and the Department of Defense Somatic Cell Processing Facility at the DRI (N00244-07-C-1529). We thank the Diabetes Research Institute Analytical Imaging Core for use of their facilities, as well as the assistance of George McNamara in image collection and processing. We also thank BioRep Technologies Inc (Miami, FL) for the fabrication of the parallel air flow bead generator used in this study.

## References

- Orive G, Hernández RM, Gascón AR, Calafiore R, Chang TMS, De Vos P, Hortelano G, Hunkeler D, Lacík I, Shapiro AMJ, Pedraz JL. Cell encapsulation: Promise and progress. *Nature Med.* 2003; 9:104–107. [PubMed: 12514721]
- Dragnet KI, Taylor C. Chemical, physical and biological properties of alginates and their biomedical implications. *Food Hydrocolloids.* 2011; 25:251–256.
- Li L, Fang Y, Vreeker R, Appelqvist I, Mendes E. Reexamining the egg-box model in calcium-alginate gels with x-ray diffraction. *Biomacromolecules.* 2007; 8:464–468. [PubMed: 17291070]
- Davis TA, Llanes F, Volesky B, Mucci A. Metal selectivity of *Sargassum* spp. And their alginates in relation to their  $\alpha$ -L-guluronic acid content and conformation. *Environ Sci Technol.* 2003; 37:261–267. [PubMed: 12564896]
- Ménard M, Dusseault J, Langlois G, Baille WE, Tam SK, Yahia LH, Zhu XX, Hallé JP. Role of protein contaminants in the immunogenicity of alginates. *J Biomed Mater Res Part B.* 2010; 93B: 333–340.
- Pokrywczynska M, Drewa T, Jundzill A, Lysik J. Alginate is not a good material for growth of rapidly proliferating cells. *Transplant Proc.* 2008; 40:1664–1667. [PubMed: 18589169]
- Augst AD, Kong HJ, Mooney DJ. Alginate hydrogels as biomaterials. *Macromol Biosci.* 2006; 6:623–633. [PubMed: 16881042]
- Breguet V, Gugerli R, Perneti M, Stockar U-v, Marison IW. Formation of microcapsules from polyelectrolyte and covalent interactions. *Langmuir.* 2005; 21:9764–9772. [PubMed: 16207064]
- Gattás-Asfura KM, Stabler CL. Chemoselective cross-linking and functionalization of alginate via Staudinger ligation. *Biomacromolecules.* 2009; 10:3122–3129. [PubMed: 19848408]
- Saxon E, Bertozzi CR. Cell surface engineering by a modified Staudinger reaction. *Science.* 2000; 287:2007–2010. [PubMed: 10720325]
- Hall KK, Gattás-Asfura KM, Stabler CL. Microencapsulation of islets within alginate/poly(ethylene glycol) gels cross-linked via Staudinger ligation. *Acta Biomaterialia.* 2011; 7:614–624. [PubMed: 20654745]
- Kaiser E, Coleseccott RL, Bossinger CD, Cook PI. Color test for detection of free terminal amino groups in the solid-phase synthesis of peptides. *Anal Biochem.* 1970; 34:595–598. [PubMed: 5443684]
- Amblard M, Fehrentz J-A, Martinez J, Subra G. Methods and protocols of modern solid phase peptide synthesis. *Mol Biotechnol.* 2006; 33:239–254. [PubMed: 16946453]
- Seifert DB, Phillips JA. Porous alginate-poly(ethylene glycol) entrapment system for the cultivation of mammalian cells. *Biotechnol Prog.* 1997; 13:569–576. [PubMed: 9336976]

15. Rokstad AM, Donati I, Borgogna M, Oberholzer J, Strand BL, Espevik T, Skjåk-Bræk G. Cell-compatible covalently reinforced beads obtained from a chemoenzymatically engineered alginate. *Biomaterials*. 2006; 27:4726–4737. [PubMed: 16750563]
16. Drury JL, Dennis RG, Mooney DJ. The tensile properties of alginate hydrogels. *Biomaterials*. 2004; 25:3187–3199. [PubMed: 14980414]
17. Zhao X, Huebsch N, Mooney DJ, Suo Z. Stress-relaxation behavior in gels with ionic and covalent crosslinks. *J Appl Phys*. 2010; 107:063509.
18. Briššová M, Lacík I, Powers AC, Anilkumar AV, Wang T. Control and measurement of permeability for design of microcapsule cell delivery system. *J Biomed Mater Res*. 1998; 39:61–70. [PubMed: 9429097]

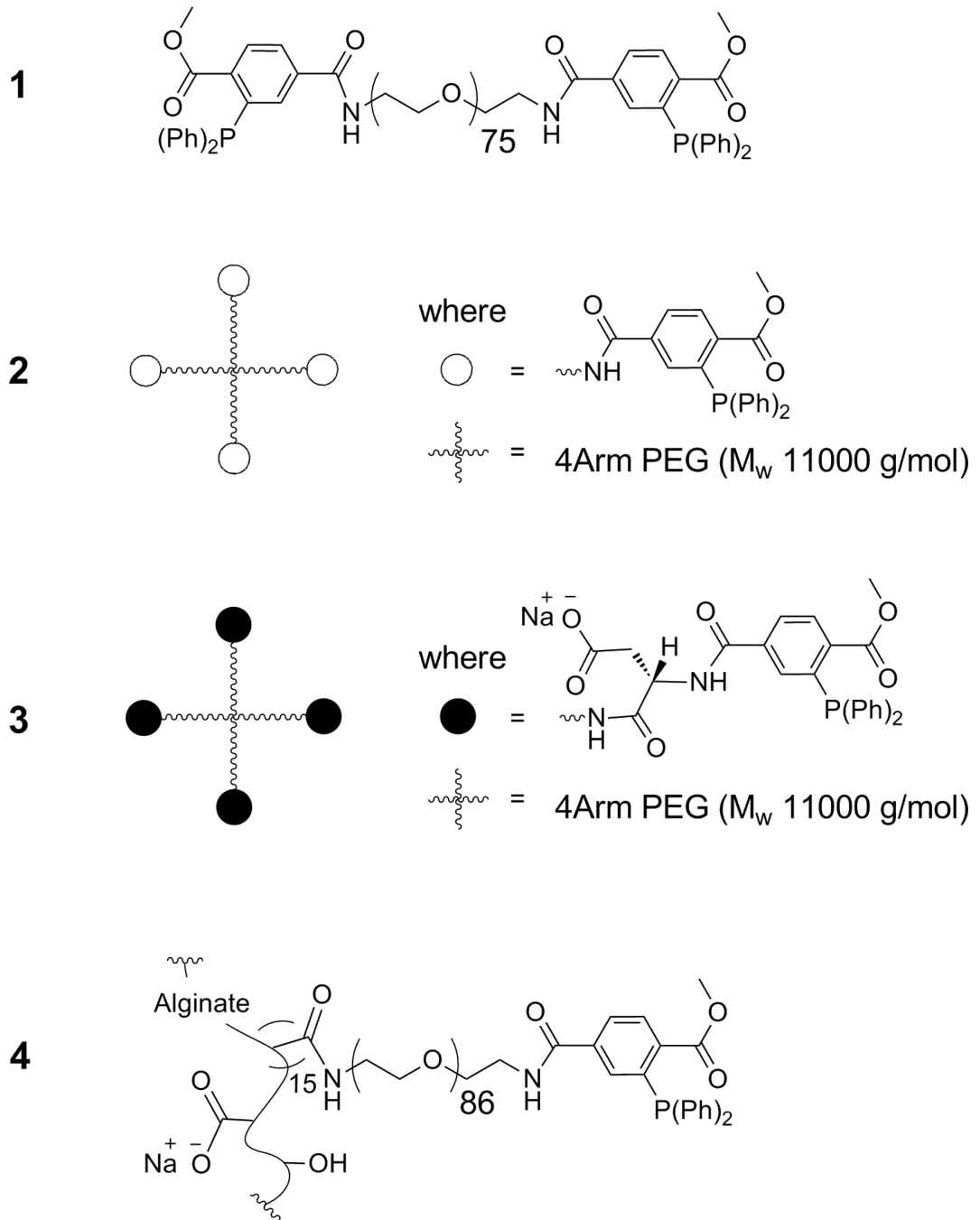


**Figure 1.**  
Structural design of crosslinkers.



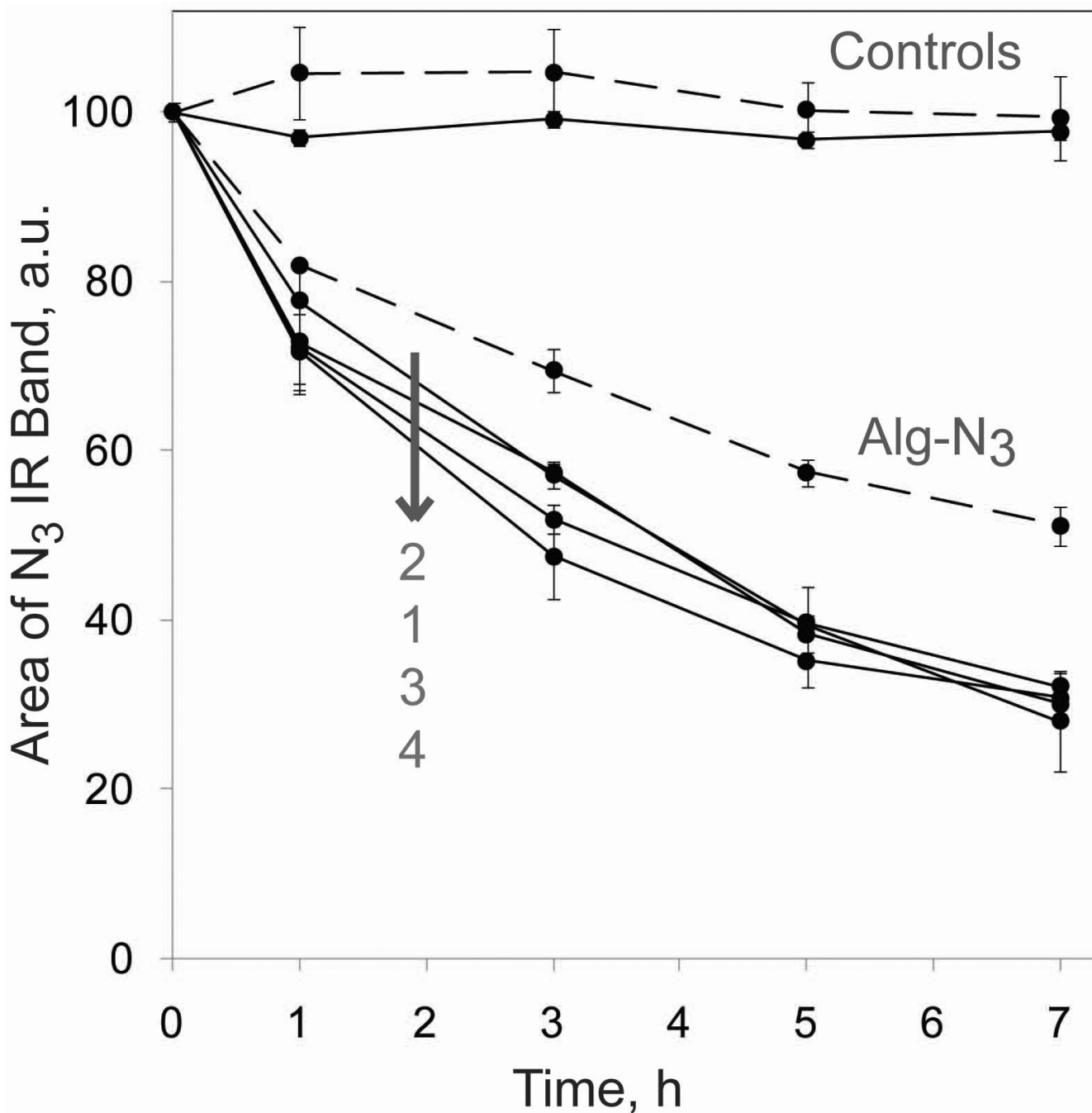


**Figure 2.** Reactivity between Alg-N<sub>3</sub> with CH<sub>3</sub>-PEG-MDT (dashed lines) and crosslinkers (1–4) with CH<sub>3</sub>-PEG-N<sub>3</sub> (solid lines), as monitored by decrease in the area of the N<sub>3</sub> IR band centered at 2121 cm<sup>-1</sup> as a function of time at 37 °C. Error bars represent standard deviations with n of 3.

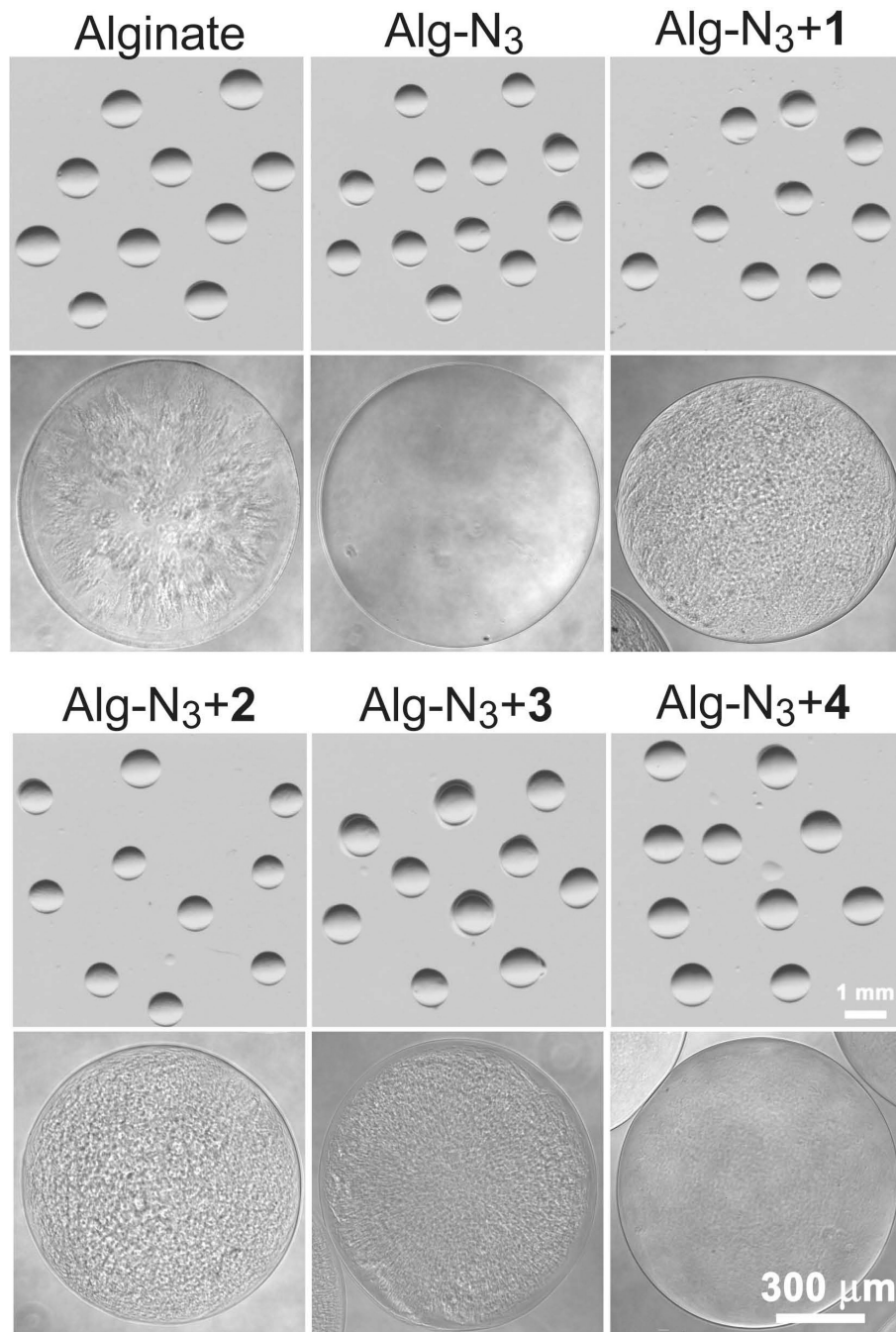


**Figure 3.** Microscopic images of the beads prepared in  $Ba^{2+}$  with the different materials at lower and higher magnification. Co-incubation time was 30, 20, 15, and 0 min for beads containing crosslinker **1**, **2**, **3**, and **4** respectively.

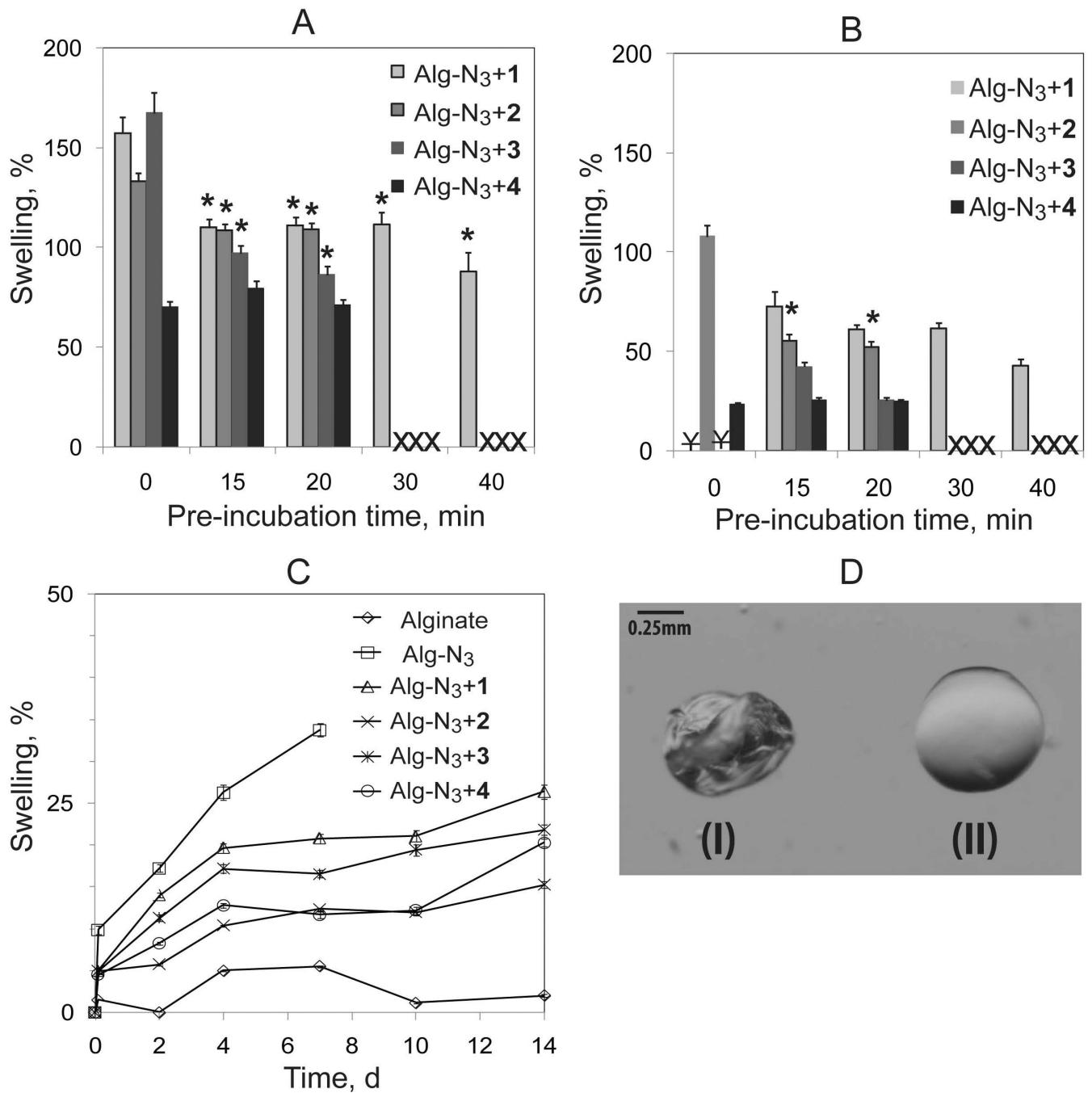


**Figure 4.** Swelling of beads consisting of alginate, Alg-N<sub>3</sub>, and Alg-N<sub>3</sub> stabilized with crosslinkers as a function of pre-incubation time, solvent, and time. A) Bead swelling following three 45 min washes with dH<sub>2</sub>O as a function of pre-incubation time; B) Bead swelling following EDTA chelation as a function of pre-incubation time; and C) Bead swelling over 14 days when incubated in DMEM. X indicates inability to fabricate beads due to high solution viscosity. ¥ indicates bead dissolution following EDTA incubation. Error bars represent standard deviations with n of 10 beads. \* indicates statistical difference between no pre-incubation time for same polymer combination. D) Microscopic images of (I) Ba<sup>2+</sup>-cross-

linked alginate bead in MOPS buffer and (II) Alg-N<sub>3</sub>+4 bead without Ba<sup>2+</sup> in MOPS after being compressed gently using two pipette tips.

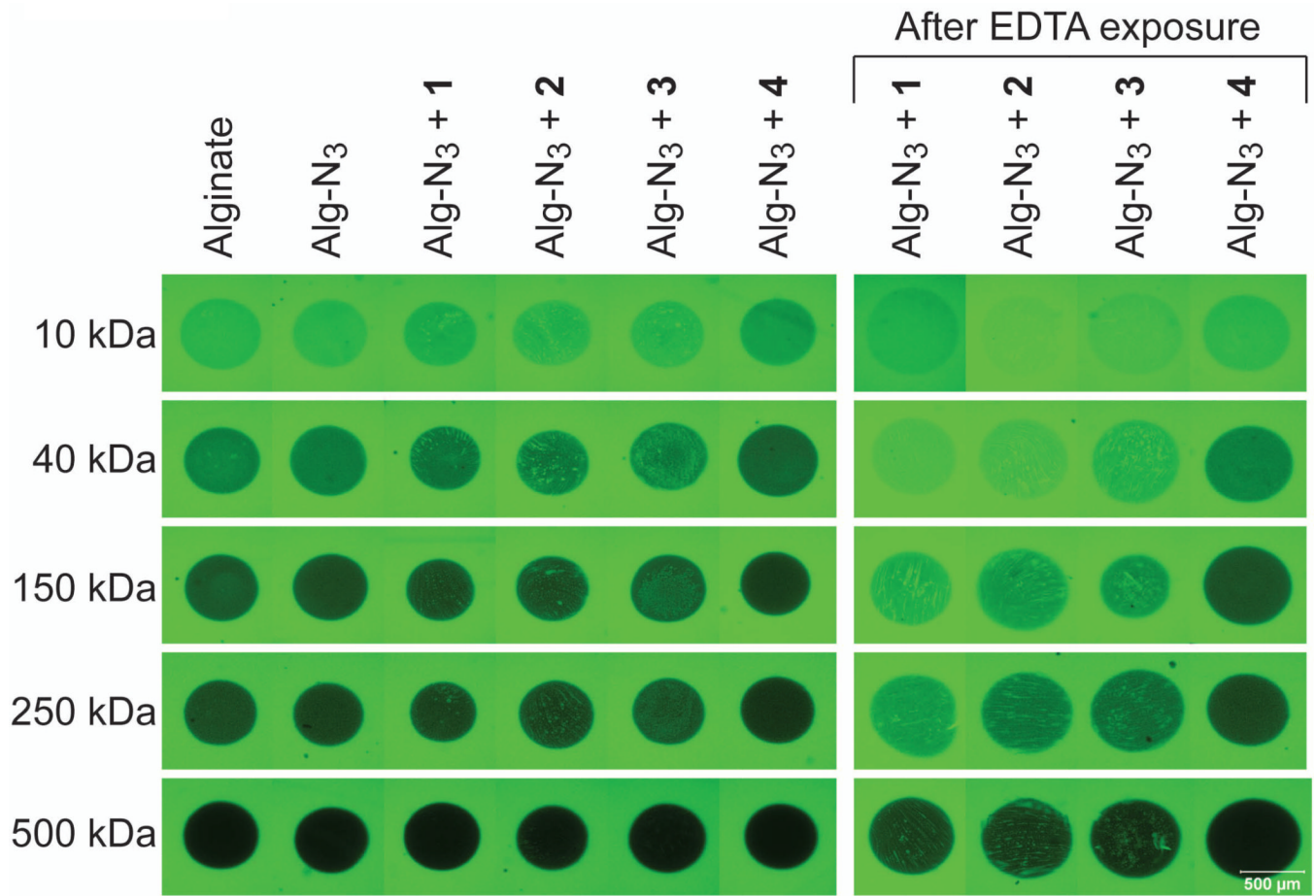


**Figure 5.**

Representative confocal images (50 μm deep planar cross-sections) of beads within FITC-dextran (0.1 mg/mL) solutions as a function of molecular weight after 2 h incubation at 37 °C in MOPS buffer (pH7.4).



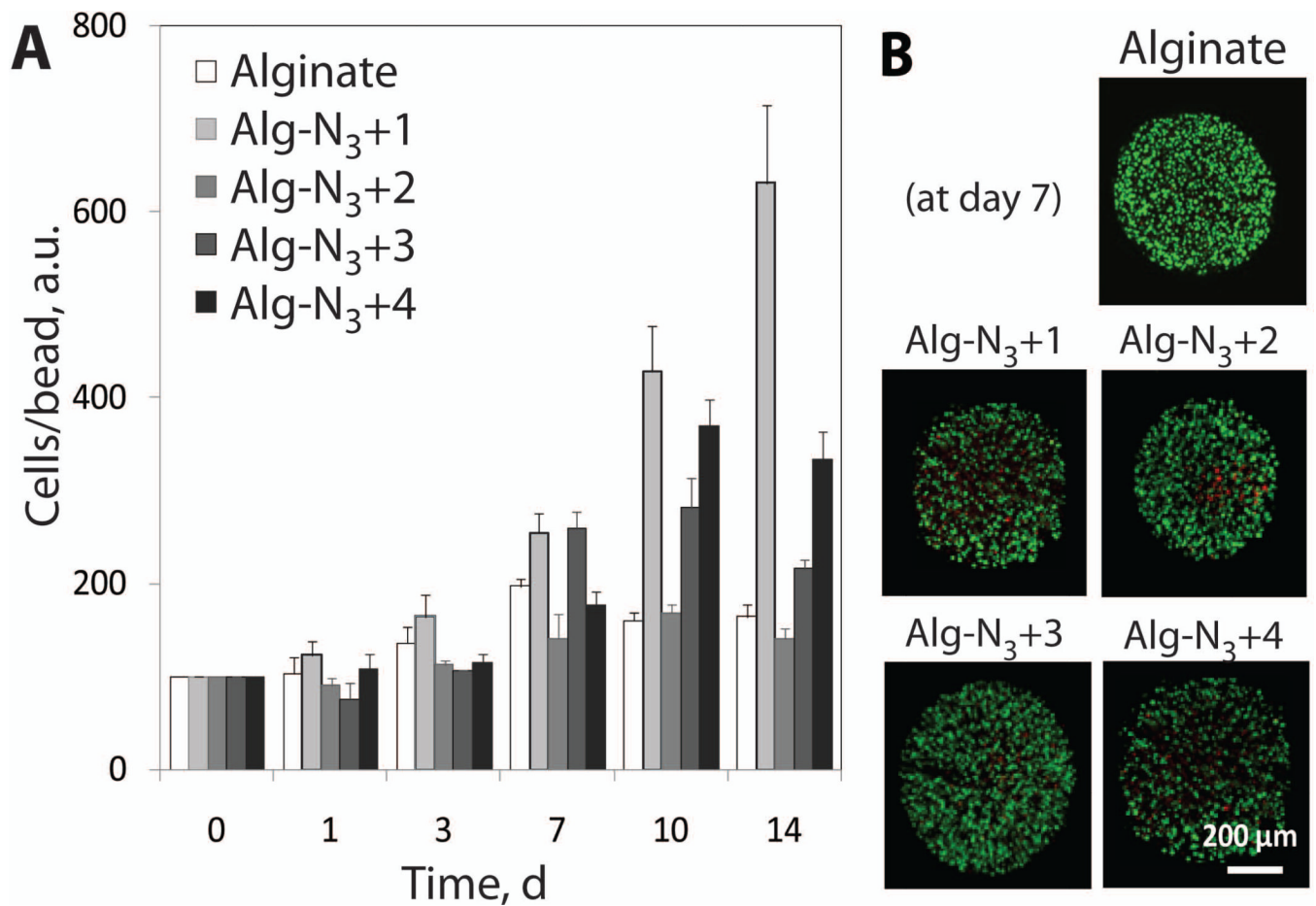


**Figure 6.**

(A) MTT assay and (B) live/dead stain as a function of time for MIN6 cells-loaded hydrogel capsules of alginate or Alg-N<sub>3</sub> stabilized with cross-linker 1–4. Error bars represent standard deviations with *n* of 30 beads. Cells/bead values as a function of time are normalized with respect to respective day zero values (a.u.), which is based on the initial average loading density of 12,000 cells per bead.

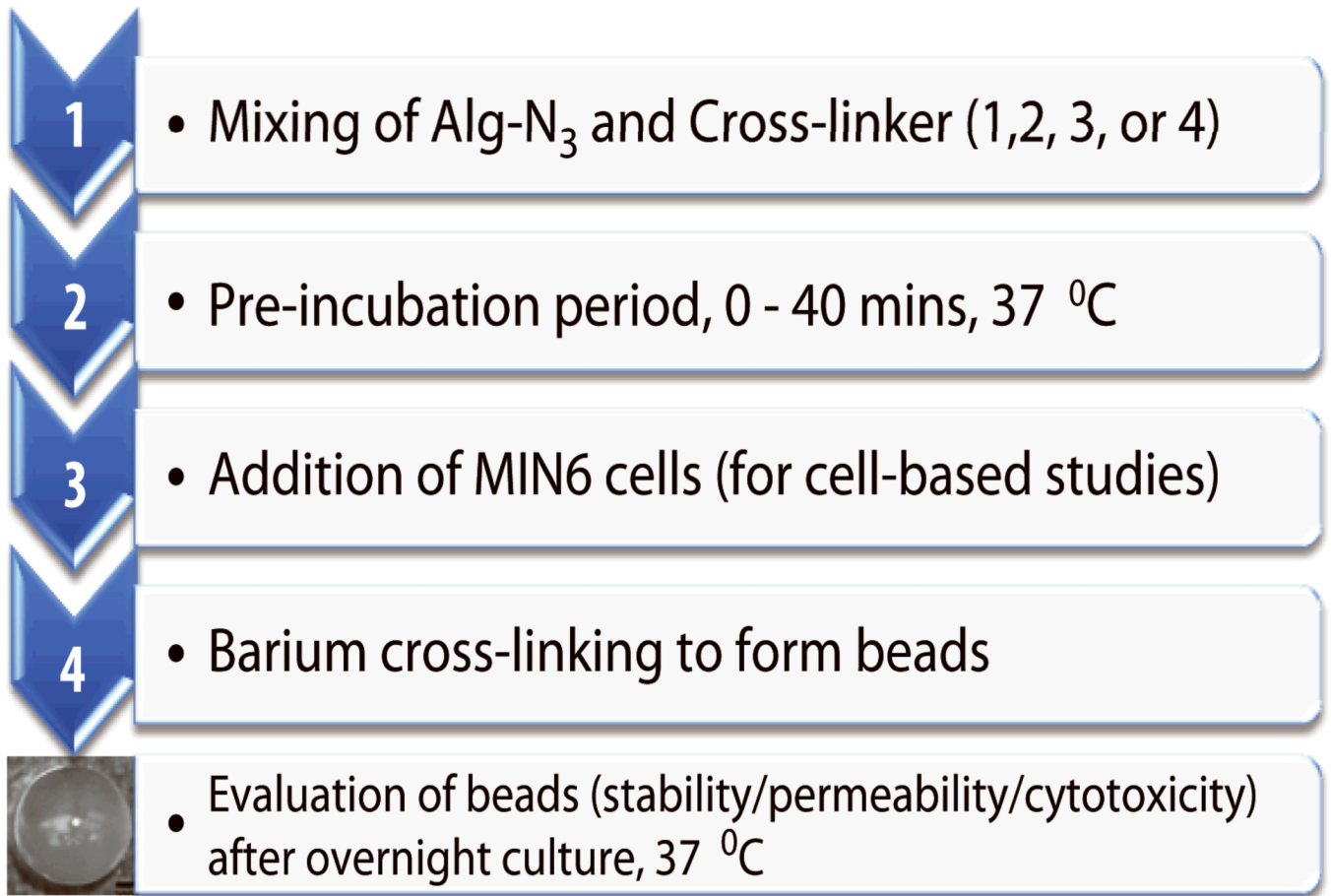
**Scheme 1.**

Diagram outlining bead fabrication/encapsulation process and tests.

**Table 1**

Characterization data for Alg-N<sub>3</sub> and cross-linkers **1–4** based on <sup>1</sup>H-NMR, FT-IR, and/or MALDI-TOF-MS analysis ( $M_w$  = weight-average molecular weight).

	$M_w$ (g/mol)	N <sub>3</sub> /material (mol ratio)	MDT/material (mol ratio)	$M_w/(N_3\text{orMDT})$ (a.u.)
Alg-N <sub>3</sub>	296,272	150	---	1.0
<b>1</b>	4,057	---	2	1.0
<b>2</b>	11,915	---	4	1.5
<b>3</b>	12,252	---	4	1.6
<b>4</b>	91,838	---	15	3.1